Investigations of Stationary MARFEs in TEXTOR-94

G.Sergienko[1], A.Pospieszczyk, J.Rapp, B.Schweer

Institut für Plasmaphysik, Forschungszentrum Jülich GmbH, EURATOM Association,
Trilateral Euregio Cluster, D-52425 Jülich, Germany
[1]Institute for High Temperatures, Association "IVTAN", Moscow, Russia

1. Introduction

A feed-back system to control the MARFE (Multi Faced Radiation From the Edge) formation for several tens of τ_p has been developed and demonstrated [1] in TEXTOR-94. The MARFE could be stabilized by a gas feed controlled via the impurity radiation from the MARFE zone - usually a CII line. The stabilization of the MARFE opened a unique possibility to investigate in detail processes inside the MARFE during its long lifetime, in particularly, to verify the interpretation of the MARFE as a result of localized plasma recycling on the inner wall [2]. The results of such investigations by means of optical diagnostic methods are presented.

2. Measurements.

The MARFE investigation has been performed on the tokamak TEXTOR-94 with a siliconized wall for the following discharge parameters: B_T= 2.24 T, I_p= 285 kA, R= 1.75 m, a= 0.46 m, $\bar{n}_e(0)$= $4 \cdot 10^{13}$ cm^{-3}. The measurements were done in deuterium discharges with 1.3 MW NBI heating (hydrogen injection). To produce a "fat" MARFE (the definition for "fat" and "thin" MARFE given in [1]) the plasma column was shifted 1 cm towards the bumper limiter. To increase the plasma density the gas puffing starts at 1.23 s in this series of the discharges shown. The MARFE appears near the midplane of the bumper limiter at 1.28 s; after then the gas puffing is controlled by the intensity of a CII(426.7nm) line from the MARFE region. The MARFE stays at the midplane position until 2.5 s; after then it moves down and disappears at about 3 s. Owing to the feedback control, such MARFE behaviour was reproducible.

Tangentially viewing CCD-cameras (color and B/W) were used in combination with interference filters to observe a full poloidal cross section at the location of the poloidal limiters. Spectral measurements in the MARFE region were performed by means of a grating spectrometer with an image intensifier CCD-camera sensitive down to 200nm. The viewing optics collected light along a tangential chord passing through the region near the bumper limiter. The image of the entrance slit of the spectrometer has been oriented radially along the equatorial plane of the torus. The spectral interval covered by the CCD-camera was about 21 nm (0.03nm per pixel) for the first diffraction order of the grating, the instrumental half width was 0.17 nm for these measurements. The radial resolution was about 0.3 cm. The time resolution of CCD-camera had a standard video output - 20 ms per half frame. The video data were digitized and stored on PC equipped with a video grabber.

A 4-channel photodiode system with interference filters viewed radially a 57x11 cm^2 area of the bumper limiter and measured simultaneously the absolute intensities of D_α(656.1nm), D_β(486.0nm), D_γ(433.93nm) and CII(426.7nm) lines with a time resolution of 0.1 ms.

There are also channels of the ECE diagnostic (time resolution 0.1ms) which received electron cyclotron radiation from the high-field side by means of an antenna mounted inside the bumper limiter. The signal of the 130 GHz electron cyclotron emission (ECE) was used

for the detection of the MARFE onset owing to a cut-off signature when the electron density in the region between antenna and emission volume (R=1.685 cm) reached a critical value of about $1.8 \cdot 10^{14} cm^{-3}$.
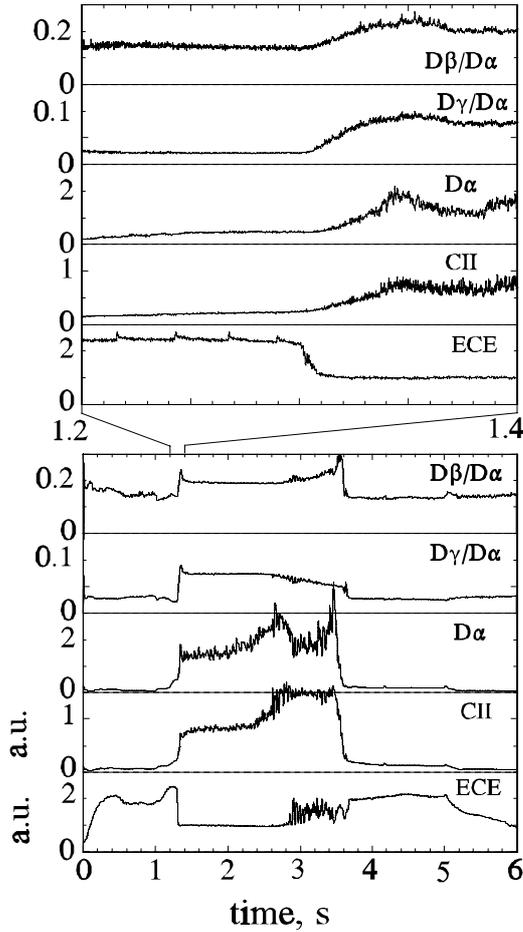
3. Experimental results and discussion.

The 130 GHz ECE signal, CII(426.7nm) line intensity, D_α intensity and intensity ratios of D_β/D_α and D_γ/D_α are shown in Fig.1. First the ECE signal drops at 1.3 s within 8 ms, then the line intensities and their ratios start to increase and reach their maxima at 1.35 s. Both ratios increase when the MARFE develops: the ratio for D_β/D_α grows from 0.13 to 0.24 and for D_γ/D_α from 0.02 to 0.09. Then the ratios decrease slightly and stabilize at 1.37 s. The D_α intensity strongly varies in time during the MARFE but the ratios are practically constant (D_β/D_α=0.2 and D_γ/D_α=0.075). Similar values for the D_γ/D_α ratio have been obtained on JET [3].

The relative line intensities of the Balmer series from D_γ to $D_{9->2}$ have been measured in the MARFE by the spectrometer mentioned above. The population densities were estimated using a MARFE size of 2x30 cm^2 and shown in Fig.2 as a function of principal quantum number. They have been evaluated at 1.1 s, 1.28 s and 2 s which correspond to periods before gas puffing, before the MARFE with gas puffing and during the stationary MARFE. It is clearly seen that the population is strongly different inside the MARFE. The population densities decrease with principal quantum number before the MARFE onset but they increase inside the MARFE. Such behaviour directly indicates that these levels are populated through a recombination process [4]. For this reason, the lines of the Balmer series cannot be used for flux measurement during a MARFE.

The profiles of the electron density and temperature inside the MARFE were evaluated from Stark broadening and the

Fig.1 Time trace of ECE, CII(426.7nm) line intensity, D_α intensity in $10^{15} phot/cm^2 \cdot sr \cdot s$, D_γ/D_α and D_β/D_α intensity ratios, #82306.
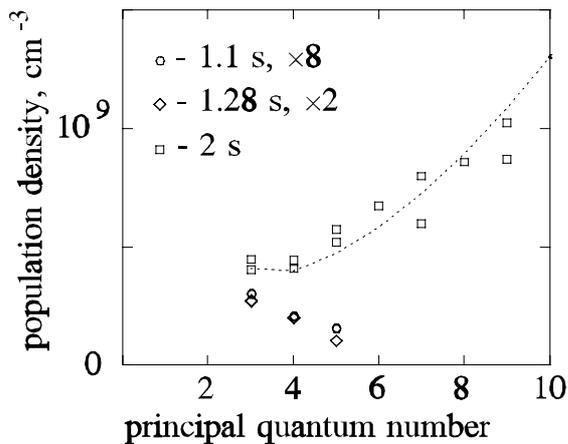

Fig.2 Population densities of deuterium levels at the bumper limiter region. The symbols indicate the measurement, dotted line - Saha equation with T_e= 1.1 eV, N_e= $2 \cdot 10^{14}$ cm^{-3}.

volume emission of the Balmer series line $D_{9->2}$(383.4nm). Abel inversion was performed to obtain the volume emission profile from the measured intensity profile as the MARFE has a toroidal symmetry and the observation chords were perpendicular to the major radius. Then, the electron density was estimated using the expression from [5]: $\Delta\lambda_{1/2}=C_nN_e^{2/3}$, were $\Delta\lambda_{1/2}$ is the full width at half maximum (FWHM) of the Stark broadened line profile. The FWHM was determined from the ratio of the total line emission to the emission in the line center. Due to NBI heating the concentration of hydrogen in the discharge was about 40%. The presence of hydrogen produced an apparent line broadening of about 0.1 nm due to the isotopic shift between the hydrogen and deuterium lines; this effect was taken into account.

An estimation shownis that the highest excited states of hydrogen and its isotopes satisfy the conditions for partial local thermodynamic equilibrium under the MARFE plasma parameters and,

Fig.3 Measured electron density and temperature profiles at high field side (HFS) and low field side (LFS) during MARFE, time 2 s, #82304.

consequently, the population density of these states is determined by the Saha equation. Neglecting impurities and taking into account that the ionization energy of the highest excited states is much smaller than the expected electron temperature the Saha equation can be rewritten to $N_e^2/N_n=3\cdot10^{21}T_e^{3/2}/n^2$, where N_n denotes the population density of the level with principal quantum number n, T_e - electron temperature in eV, N_e and N_n in cm^{-3}. The profiles of the plasma parameters in the MARFE evaluated by this procedure are shown on Fig.3 together with profiles measured on the low field side by a thermal helium beam diagnostic. The electron density inside the MARFE reaches values of about $2\cdot10^{14}$cm^{-3} whereas the electron temperature drops to about 1.1 eV. This result is in good agreement with the measured population density distribution seen in Fig.2 where the dash line indicates the population distribution calculated with the help of Saha-Boltzman equation for these plasma parameters. An analog measurement inside a "thin" MARFE yields an electron density of about $6\cdot10^{13}$cm^{-3} and the electron temperature of about 2.8 eV.

The volume emissivities of CII(426.7nm), CIII(418.7nm) and D_γ(434.05nm) lines

Fig.4 Volume emission profiles of D_γ, CII(426.7nm) and CIII(418.7nm) lines from HFS during MARFE, time 2s, #82302,#82306.

were also measured and shown in Fig.4. It is seen that the maxima of the CIII and CII emissions are shifted toward the plasma center with respect to the maximum of the D_γ
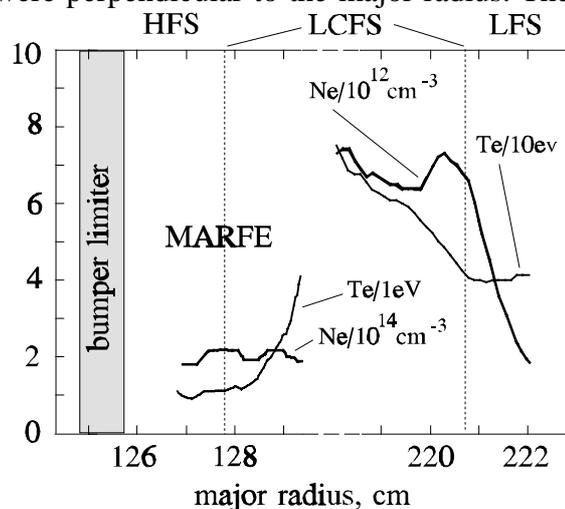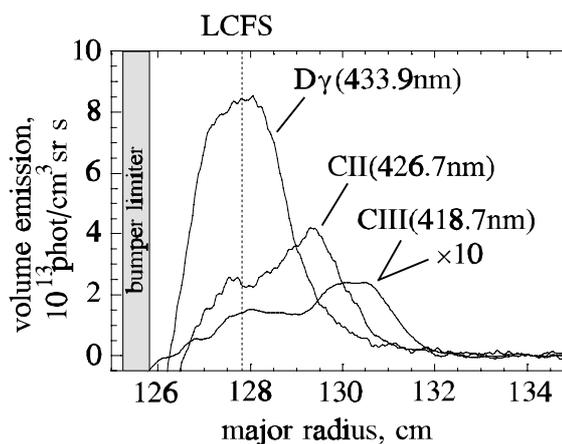
emission. Usually, an increase of plasma density near the surface is accompanied by the enhancement of the molecular re-emission [6]. During the MARFE an increase of emission from CH, C_2 molecules 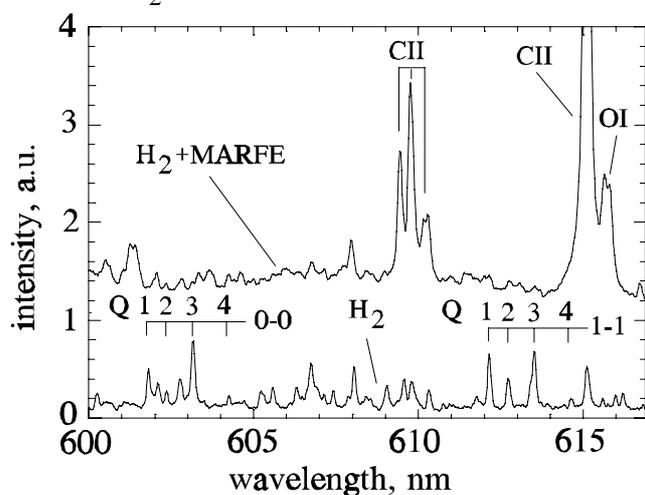was observed but not so significant as expected. This emission originates from a narrow layer about 0.5 cm close to the bumper limiter surface. The molecular deuterium emission was not seen. To distinguish the reasons of this reduction, molecular hydrogen was puffed through the hole at the midplane of the bumper limiter. The spectra recorded in the range of the Fulcher band of molecular hydrogen during gas puffing without and with MARFE are shown in Fig.5. The Fulcher band emission drops strongly (at least 10 times) inside the MARFE and is practically invisible on the continuum radiation. The reduction of the Fulcher band emissivity under such plasma parameters is in a good agreement with a prediction of a collisional-radiative model for molecular hydrogen developed by [7]. Additionally, charge-exchange between hydrogen (deuterium) molecules and ions can also essentially reduce the photon emission of these molecules.

Fig.5 Spectra measured during hydrogen puffing from the bumper limiter side without and with MARFE.

4. Conclusions

$T_e \approx 3$ eV $N_e \approx 6 \cdot 10^{13} cm^{-3}$ and $T_e \approx 1$ eV $N_e \approx 2 \cdot 10^{14} cm^{-3}$ respectively were measured inside a "thin" and a "fat" MARFE.

In the MARFE the excited levels of deuterium atoms with $n > 2$ are mainly populated via recombination and cannot be used for measurements of the neutral particle flux.

The emissivity of the Fulcher band of molecular hydrogen strongly reduces for MARFE plasma conditions so that the molecular hydrogen (deuterium) flux could not be measured due to the strong continuum background.

References

[1]   U.Samm, M.Brix, F.Durodie et al., J.Nucl.Matter, **266-269** (1999) 666

[2]   M.Z.Tokar', J.Rapp, D.Reiser et al., J.Nucl.Matter, **266-269** (1999) 958

[3]   G.M.McCracken, M.F.Stamp, R.D.Monk et al., Nucl.Fusion, Vol.38, No. 4 (1998) 619

[4]   D.Lumma, J.L.Terry and B.Lipschultz, Phys.Plasmas, Vol.4, No.7 (1997) 2555

[5]   B.L.Welch, H.R.Griem, J.Terry et al., Phys.Plasmas, Vol.2, No.11 (1995) 4246

[6]   A.Pospieszczyk, Ph. Mertens, G.Sergienko et al., J.Nucl.Matter, **266-269** (1999) 138

[7]   P.T.Greenland, private communication